

1 **Scaling diagnostics in times of COVID-19: Colorimetric Loop-mediated Isothermal**  
2 **Amplification (LAMP) assisted by a 3D-printed incubator for cost-effective and**  
3 **scalable detection of SARS-CoV-2**

4

5 Everardo González-González<sup>1,2</sup>, Itzel Montserrat Lara-Mayorga<sup>1,3</sup>, Felipe Yee-de León<sup>4</sup>,  
6 Andrés García-Rubio<sup>1,3</sup>, Carlos Ezio Garciaméndez-Mijares<sup>1,3,5</sup>, Gilberto Emilio-Guerra-  
7 Alvarez<sup>1,3</sup>, Germán García-Martínez<sup>1,3,5</sup>, Juan Aguayo<sup>1,3</sup>, Iram Pablo Rodríguez-Sánchez<sup>6,7</sup>,  
8 Yu Shrike Zhang<sup>5</sup>, Sergio Omar Martínez-Chapa<sup>3</sup>, Grissel Trujillo-de Santiago<sup>1,3,\*</sup>, Mario  
9 Moisés Alvarez<sup>1,2\*</sup>

10

11 <sup>1</sup> Centro de Biotecnología-FEMSA, Tecnológico de Monterrey, CP 64849, Monterrey, NL,  
12 México

13 <sup>2</sup> Departamento de Bioingeniería, Tecnológico de Monterrey, CP 64849, Monterrey, NL,  
14 México

15 <sup>3</sup> Departamento de Ingeniería Mecánica y Eléctrica, Tecnológico de Monterrey, CP  
16 64849, Monterrey, NL, México

17 <sup>4</sup> Delee Corp. Mountain View 94041, CA, USA

18 <sup>5</sup> Division of Engineering in Medicine, Department of Medicine, Brigham and Women's  
19 Hospital, Harvard Medical School, Cambridge 02139, MA, USA

20 <sup>6</sup> Alfa Medical Center, Guadalupe, CP 67100, NL, México.

21 <sup>7</sup> Universidad Autónoma de Nuevo León, Facultad de Ciencias Biológicas, Laboratorio de  
22 Fisiología Molecular y Estructural. 66455, San Nicolás de los Garza, NL, México.

23 \*Corresponding authors. E-mails: [mario.alvarez@tec.mx](mailto:mario.alvarez@tec.mx); [grissel@tec.mx](mailto:grissel@tec.mx);

24

25

Submitted to *Nature Biomedical Engineering*

## 26 **Abstract**

27 By the first week of April 2020, more than 3,400,000 positive cases of COVID-19 and  
28 more than 230,000 deaths had been officially reported worldwide. While developed  
29 countries such as the USA, Italy, England, France, Spain, and Germany struggle to mitigate  
30 the propagation of SARS-CoV-2, the COVID-19 pandemic arrived in Latin America, India,  
31 and Africa—territories in which the mounted infrastructure for diagnosis is greatly  
32 underdeveloped. An actual epidemic emergency does not provide the required timeframe  
33 for testing new diagnostic strategies; therefore, the first line of response must be based on  
34 commercially and readily available resources. Here, we demonstrate the combined use of a  
35 three-dimensional (3D)-printed incubation chamber for commercial Eppendorf PCR tubes,  
36 and a colorimetric embodiment of a loop-mediated isothermal amplification (LAMP)  
37 reaction scheme for the detection of SARS-CoV-2 nucleic acids. We used this strategy to  
38 detect and amplify SARS-CoV-2 DNA sequences using a set of in-house designed  
39 initiators that target regions encoding the N protein. We were able to detect and amplify  
40 SARS-CoV-2 nucleic acids in the range of ~625 to  $2 \times 10^5$  DNA copies by this  
41 straightforward method. The accuracy and simplicity of this diagnostics strategy may  
42 provide a cost-efficient and reliable alternative for use during the COVID-19 pandemics,  
43 particularly in underdeveloped regions where the availability of RT-qPCR instruments may  
44 be limited. Moreover, the portability, ease of use, and reproducibility of this strategy make  
45 it a reliable alternative for deployment of point-of-care SARS-CoV-2 detection efforts  
46 during the pandemics.

47

48 **Key words:** LAMP, point-of-care, SARS-CoV-2, COVID-19, diagnostic, portable,  
49 isothermal nucleic acid amplification

50

## 51 **Introduction**

52 By the end of the first week of May 2020, more than 3.4 million positive cases of COVID-  
53 19 were officially reported across the globe[1]. Even developed countries, such as the USA,  
54 England, France, and Germany, are struggling to mitigate the propagation of SARS-CoV-2

55 by implementing social distancing and widespread testing. Less developed regions, such as  
56 Latin America, India, and Africa, are now experiencing the arrival of COVID-19, but  
57 these—territories are woefully lacking in the finances or the mounted infrastructure for  
58 diagnosis of this pandemic infection. Rapid and massive testing of thousands of possibly  
59 infected subjects has been an important component of the strategy of the countries that are  
60 effectively mitigating the spreading of COVID-19 among their populations (i.e., China[2],  
61 South Korea [3], and Singapore [4]). By comparison, developing countries with high  
62 demographic densities, such as México [5], India [6], or Brazil [7], may not be able to  
63 implement a sufficient number of centralized laboratories for rapid large-scale testing for  
64 COVID-19.

65 Many methodologies have been proposed recently to deliver cost-effective diagnosis (i.e.,  
66 those based on immunoassays [8–11] or specific gene hybridization assisted by CRISPR-  
67 Cas systems [12–14]). While immunoassays are an accurate and efficacious tool for  
68 assessing the extent of the infection for epidemiological studies [15], their usefulness is  
69 limited to the identification of infected subjects during early phases of infection [11,16], a  
70 critical period for infectiveness. For instance, experimental evidence collected from a small  
71 number of COVID-19 patients (9 subjects) showed that 100% of them produced specific  
72 immunoglobulins G (IgGs) for SARS-CoV-2 within two weeks of infection, but only 50%  
73 of them did during the first week post infection [17].

74 Nucleic acid amplification continues to be the gold standard for the detection of viral  
75 diseases in the early stages [18–22], and very small viral loads present in symptomatic or  
76 asymptomatic patients can be reliably detected using amplification based technics, such as

77 polymerase chain reaction (PCR) [23–25], recombinase polymerase amplification  
78 (RPA)[26], and loop-mediated isothermal amplification (LAMP) [27–29].

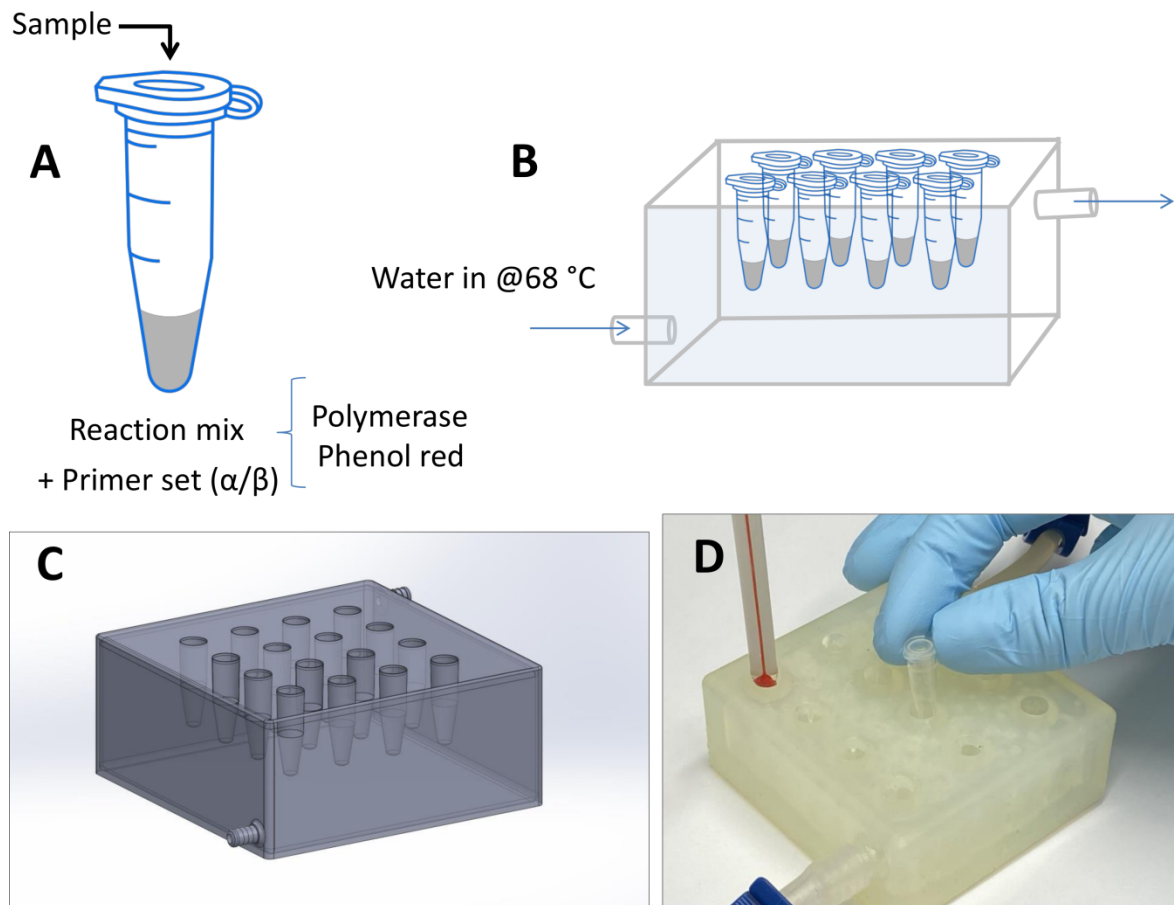
79 During the last two pandemic events with influenza A/H1N1/2009 and COVID-19, the  
80 Centers for Disease Control and Prevention (CDC) and the World Health Organization  
81 (WHO) recommended real-time quantitative PCR (RT-qPCR) methods as the gold standard  
82 for official detection of positive cases[16,30]. However, the reliance on RT-qPCR often  
83 leads to dependence on centralized laboratory facilities for testing [16,30–33]. To resolve  
84 this drawback, isothermal amplification reaction schemes (i.e., LAMP and RPA) have been  
85 proposed as alternatives to PCR-based methods and devices for point-of-care settings  
86 [32,34,35]. The urgency of using reliable molecular-based POC methods for massive  
87 diagnostic during epidemiological emergencies has become even more evident during the  
88 current COVID-19 pandemics [30,36,37].

89 In these times of COVID-19 [38], scientists and philanthropists around the globe have  
90 worked expeditiously on the development of rapid and portable diagnostics for SARS-  
91 CoV-2. Several reports have demonstrated the use of colorimetric LAMP-based methods  
92 for diagnosis of pandemic COVID-19 [39–44]. Some of these reports (currently available  
93 as preprints) use phenol red, a well-known pH indicator, to assist in the visual  
94 discrimination between positive and negative samples [39,40].

95 In this study, we demonstrate the use of a simple embodiment of a colorimetric LAMP  
96 protocol for the detection and amplification of synthetic samples of SARS-CoV-2, the  
97 causal viral agent of COVID-D. In this LAMP-based strategy, also assisted by the use of  
98 phenol red, sample incubation is greatly facilitated by the use of a three-dimensional (3D)-  
99 printed incubator connected to a conventional water circulator, while discrimination

100 between positive and negative samples is achieved by visual inspection. We quantitatively  
101 analyze differences in color between positive and negative samples using color  
102 decomposition and analysis in the color CIELab space[45]. Moreover, we compare the  
103 sensibility of this LAMP colorimetric method versus PCR protocols. This simple strategy is  
104 potentially adequate for the fast deployment of diagnostic efforts in the context of COVID-  
105 19 pandemics.

106



107

108 **Figure 1. Experimental setup.** (A) Commercial 200 microliter Eppendorf PCR tubes, and (B) a  
109 3D-printed incubator was used in amplification experiments of samples containing the synthetic  
110 SARS-CoV-2 nucleic acid material. (C) 3D CAD model of the LAMP reaction incubator. (D)  
111 Actual image of the Eppendorf tube incubator connected to a conventional water circulator.

112 **Rationale**

113 We have developed a simple diagnostic method for the detection of SARS-CoV-2, the  
114 causal agent of COVID-19. The rationale underlying this strategy is centered on achieving  
115 the simplest possible integration of easily available reagents, materials, and fabrication  
116 techniques to facilitate fast and massive implementation during the current COVID-19  
117 pandemics in low- or middle-income regions.

118 This method is based on the amplification of the genetic material of SARS-CoV-2 using  
119 LAMP. The amplification is conducted using a commercial reaction mix in commercial and  
120 widely available 200  $\mu$ L Eppendorf PCR tubes. Moreover, we have designed and fabricated  
121 a simple 3D-printed chamber (Figure 1) for incubation of the Eppendorf tubes and to enable  
122 LAMP at high temperatures (50–65 °C) and extended times (up to 1 h). We show that this  
123 incubation chamber, when connected to a conventional water recirculator, enables the  
124 successful amplification of positive samples (i.e., samples containing SARS-CoV-2 nucleic  
125 acids).

126 This incubation chamber is one of the key elements that enable rapid and widespread  
127 implementation of this diagnostic method at low cost. This 3D-printed incubator can be  
128 rapidly printed using standard SLA printers widely available in markets worldwide.  
129 Standard 3D-printing resins can be used. The availability of the original AutoCAD files  
130 (included here as supplemental material) enables fast modification/optimization of the  
131 design for accommodation of a larger number of samples or larger or smaller tubes,  
132 adaptation to any available hoses (tubing), and possible incorporation of an on-line color-  
133 reading system. Indeed, all this is consistent with the main rationale of our proposed  
134 diagnostic strategy for pandemic COVID-19: To enabling a fast and feasible response using

135 widespread, distributed, and scalable diagnostics fabricated with widely available  
136 resources.

137 In the following section, we briefly discuss the mechanisms of amplification and visual  
138 discrimination between positive and negative samples.

139

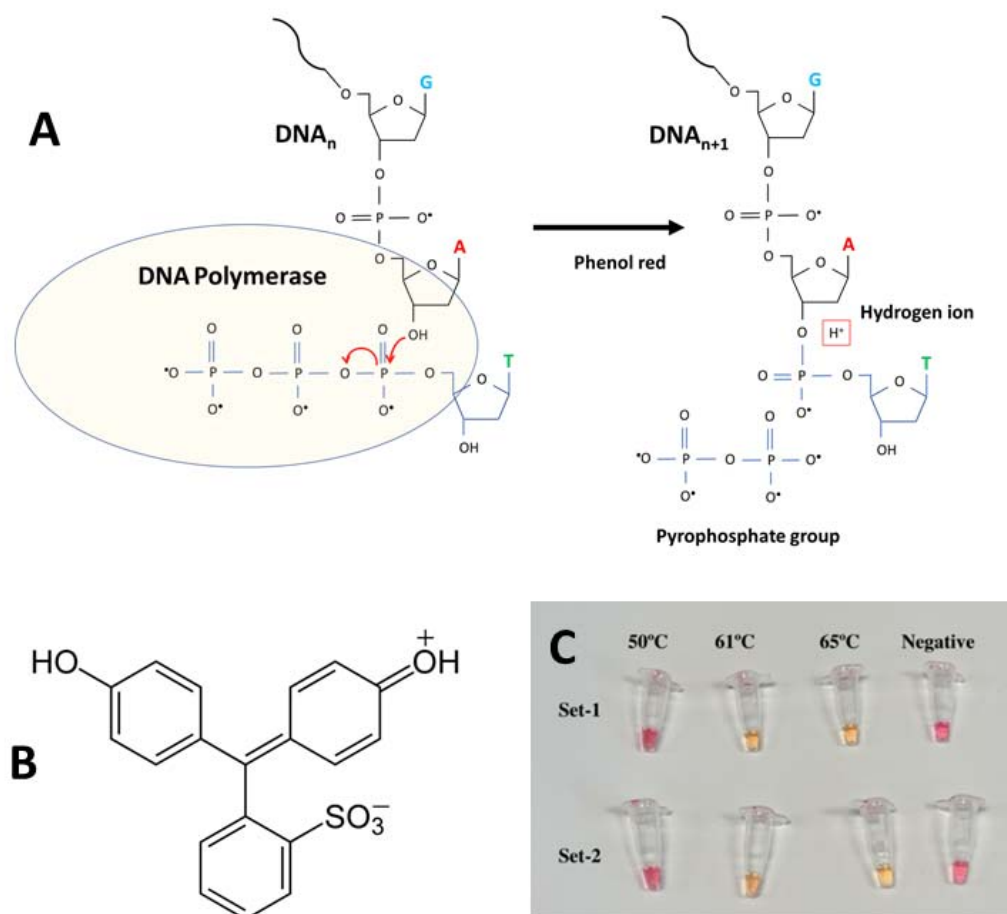
#### 140 **Colorimetric LAMP amplification**

141 The presence of phenol red within the LAMP reaction mix allows for naked-eye  
142 discrimination between positive and negative samples (Figure 2). The reaction mix is  
143 coupled with the pH color transition of phenol red, a widely used pH indicator, which shifts  
144 in color from red to yellow at pH 6.8. During LAMP amplification, the pH of the reaction  
145 mix continuously evolves from neutrality to acidic values as protons are produced [27,47].

146 The mechanism of production of hydrogen ions ( $H^+$ ) during amplification in weakly  
147 buffered solutions has been described [47]. DNA polymerases incorporate a  
148 deoxynucleoside triphosphate into the nascent DNA chain. During this chemical event, a  
149 pyrophosphate moiety and a hydrogen ion are released as byproducts (Figure 2A). This  
150 release of hydrogen ions is quantitative, according to the reaction scheme illustrated in  
151 Figure 2. The caudal of  $H^+$  is high, since it is quantitatively proportional to the number of  
152 newly integrated dNTPs. In fact, the quantitative production of  $H^+$  is the basis of previously  
153 reported detection methods, such as the semiconductor sequencing technology operating in  
154 Ion Torrent sequencers[48]. In the initially neutral and weakly buffered reaction mixes, the  
155 production of  $H^+$  during LAMP amplification progressively and rapidly shifts the pH across  
156 the threshold of phenol red (Figure 2B).

157 Moreover, the pH shift is clearly evident to the naked eye, thereby freeing the user from  
158 reliance on spectrophotometric instruments and facilitating simple implementation during

159 emergencies (Figure 2C). Images in Figure 2C show representative colors of the  
160 amplification reaction mixes contained in Eppendorf PCR tubes after incubation for 30  
161 min. Three different incubation temperatures were tested (50, 60, and 65 °C) and two  
162 different sets of LAMP-primers ( $\alpha$  and  $\beta$ ) were used (Table 1).



163

164 **Figure 2. Initiators and pH indicator for SARS-Co2 detection using a colorimetric LAMP**  
165 **method.** (A) The LAMP reaction scheme. (B) Chemical structure of phenol red. (C) Two different  
166 sets of LAMP primers were used for successfully targeting a gene sequence encoding the SARS-  
167 Co2 N protein. Successful targeting and amplification are clearly evident to the naked eye: positive  
168 samples shift from red to yellow.

169

170



171 **Table 1. Primer sequences used in LAMP amplification experiments.** Two different sets of  
 172 primers were used, directed at the RNA sequence encoding the N sequence of the SARS-CoV-2.

Set	Description	Primers Sequence (5'>3')
Primer set $\alpha$	2019-nCoV 1-F3	TGGACCCCAAATCAGCG
	2019-nCoV 1-B3	GCCTTGTCTCGAGGGAAT
	2019-nCoV 1-FIP	CCACTGCGTTCTCCATTCTGGTAAATGCACCCCGCATTACG
	2019-nCoV 1-BIP	CGCGATCAAAACAACGTCGGCCCTTGCCATGTTGAGTGAGA
	2019-nCoV 1-LF	TGAATCTGAGGGTCCACCAA
	2019-nCoV 1-LB	TTACCCAATAATACTGCGTCTTGGT
Primer set $\beta$	2019-nCoV 2-F3	CCAGAATGGAGAACGCAGTG
	2019-nCoV 2-B3	CCGTCACCACCACGAATT
	2019-nCoV 2-FIP	AGCGGTGAACCAAGACGCAGGGCGCGATCAAAACAACG
	2019-nCoV 2-BIP	AATTCCCTCGAGGACAAGGCGAGCTCTTCGGTAGTAGCCAA
	2019-nCoV 2-LF	TTATTGGGTAAACCTTGGGGC
	2019-nCoV 2-LB	TAACACCAATAGCAGTCCAGATGA

173

174

175 Both sets of primers performed equivalently, at least based on visual inspection, in the three  
 176 temperature conditions tested. Discrimination between positive and negative controls is  
 177 possible using only the naked eye to discern the reaction products from amplifications  
 178 conducted at 60 and 65 °C. No or negligible amplification was evident at 50 °C or in the  
 179 control group.

180 Furthermore, we were able to successfully discriminate between positive and negative  
 181 samples using LAMP reaction mix already added with primers and kept at room  
 182 temperature or 4 °C for 24, 48, 72, and 96 h (Figure S3). The stability of the reaction, the  
 183 isothermal nature of the amplification process, and its independence from specialized

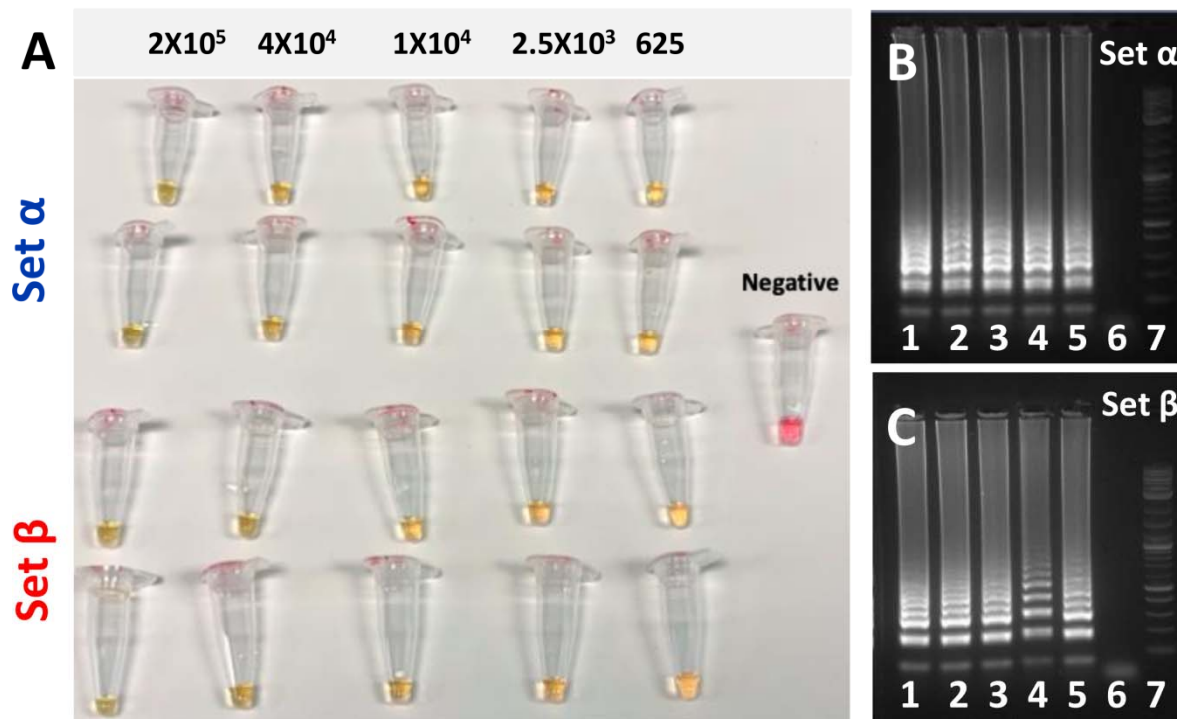
184 equipment greatly simplifies the logistic of implementation of this diagnostic method  
185 outside centralized labs.

186

### 187 **Analysis of sensitivity**

188 We conducted a series of experiments to assess the sensitivity of the LAMP reactions in the  
189 3D-printed incubation chamber using the two sets of primers ( $\alpha$  and  $\beta$ ; Table 1). The  
190 amplification proceeds with sufficient quality to also allow proper visualization of the  
191 amplification products in electrophoresis gels, even at low nucleic acid concentrations. We  
192 observed that amplification proceeded successfully in a wide range of viral loads, from 625  
193 to  $5 \times 10^5$  copies in experiments using synthetic SARS-CoV-2 nucleic acid material (Figure  
194 3A).

← Increasing viral copies →



195

196 **Figure 3. Two different sets of LAMP-primers were used for successfully targeting of a gene**  
197 **sequence encoding the SARS-Co2 N protein. (A) LAMP primer sets  $\alpha$  and  $\beta$  both enable the**

198 amplification of synthetic samples of SARS-CoV-2 nucleic acids in a wide range of template  
199 concentrations, from 625 to  $2.0 \times 10^5$  DNA copies of SARS-CoV-2 when incubated for 50 minutes  
200 at a temperature range from 60 to 65 °C. (B, C) Agarose gel electrophoresis of DNA amplification  
201 products generated by targeting two different regions of the sequence coding for SARS-Co2 N  
202 protein. Two different primer sets were used: (B) primer set  $\alpha$ , and (C) primer set  $\beta$ . The initial  
203 template amount was gradually decreased from left to right:  $2.0 \times 10^5$  DNA copies (lane 1),  $4.0 \times$   
204  $10^4$  copies, (lane 2),  $1.0 \times 10^4$  copies (lane 3),  $2.5 \times 10^3$  copies (lane 4), 625 copies (lane 5), negative  
205 control (lane 6), and molecular weight ladder (lane 7).

206

207 We clearly observed amplification in samples containing as few as 625 viral copies after  
208 incubation times of 5 min at 65 °C. If we put this range into a proper clinical context, the  
209 actual viral load of COVID-19 in nasal swabs from patients has been estimated to fall  
210 within the range of  $10^5$  to  $10^6$  viral copies per mL [49]. Discrimination between positive  
211 and negative samples (controls) can be clearly established by the naked eye in all reactions  
212 incubated for 50 min, regardless of the number of viral copies present. In addition, we did  
213 not observe any non-specific amplification in negative samples (i.e., containing synthetic  
214 genetic material from EBOV) incubated for 50 min at 65 °C. Indeed, the identification and  
215 amplification of SARS-CoV-2 synthetic material is feasible in samples that contained ~62.5  
216 viral copies using this LAMP strategy (Figure S3) and incubation times of 50–60 min.

217 We corroborated the amplification by visualizing LAMP products with gel electrophoresis  
218 for the different viral loads tested. Figures 3B, C show agarose gels of the amplification  
219 products of each one of the LAMP experiments, where two different sets of primers ( $\alpha$  and  
220  $\beta$ ) were used to amplify the same range of concentrations of template (from 625 to  $2 \times 10^5$   
221 synthetic viral copies). We were able to generate a visible array of bands of amplification  
222 products, a typical signature of LAMP, for both LAMP primer sets and across the whole

223 range of synthetic viral loads. Indeed, both primer sets rendered similar amplification  
224 profiles.

225 In summary, using the primers and methods described here, we were able to consistently  
226 detect the presence of SARS-CoV-2 synthetic nucleic acids. We have used a simple 3D-  
227 printed incubator, connected to a water circulator, to conduct LAMP. We show that, after  
228 only 30 min of incubation, samples containing a viral load in the range of  $10^4$  to  $10^5$  copies  
229 could be clearly discriminated from negative samples by visual inspection with the naked  
230 eye (Figure 2C). Samples with a lower viral load were clearly discriminated when the  
231 LAMP reaction was incubated for 50 min. Incubation periods of up to 1 h at 68 °C did not  
232 induced false positives and were able to amplify as few as ~62 copies of SARS-CoV-2  
233 synthetic genetic material. These results are consistent with those of other reports in which  
234 colorimetric LAMP, assisted by phenol red, has been used to amplify SARS-COV-2  
235 genetic material [39,40].

236 We observe 0 false positive cases in experiments where synthetic samples containing  
237 EBOV genetic material were incubated at 65 °C for 1 h.

238 In the current context of the COVID-19 pandemics, the importance of communicating this  
239 result does not reside in its novelty but in its practicality. Some cost considerations follow.  
240 While the market value of a traditional RT-qPCR apparatus (the current gold standard for  
241 COVID-19 diagnostics) is in the range of 10,000 to 40,000 USD, a 3D-printed incubator,  
242 such as the one described here (Figure S1,S2; Supplementary file S1), could be fabricated  
243 for under 200 USD at any 3D printer shop. This difference is significant, especially during  
244 an epidemic or pandemic crisis when rational investment of resources is critical. While the  
245 quantitative capabilities of testing using an RT-qPCR platform are undisputable, the  
246 capacity of many countries to rapidly, effectively, and massively establish diagnostic

247 centers based on RT-qPCR is questionable. The current pandemic scenarios experienced in  
248 the USA, Italy, France, and Spain, among others, have crudely demonstrated that  
249 centralized labs are not an ideal solution during emergencies. Portable diagnostic systems  
250 may provide a vital flexibility and speed of response that RT-qPCR platforms cannot  
251 deliver.

252

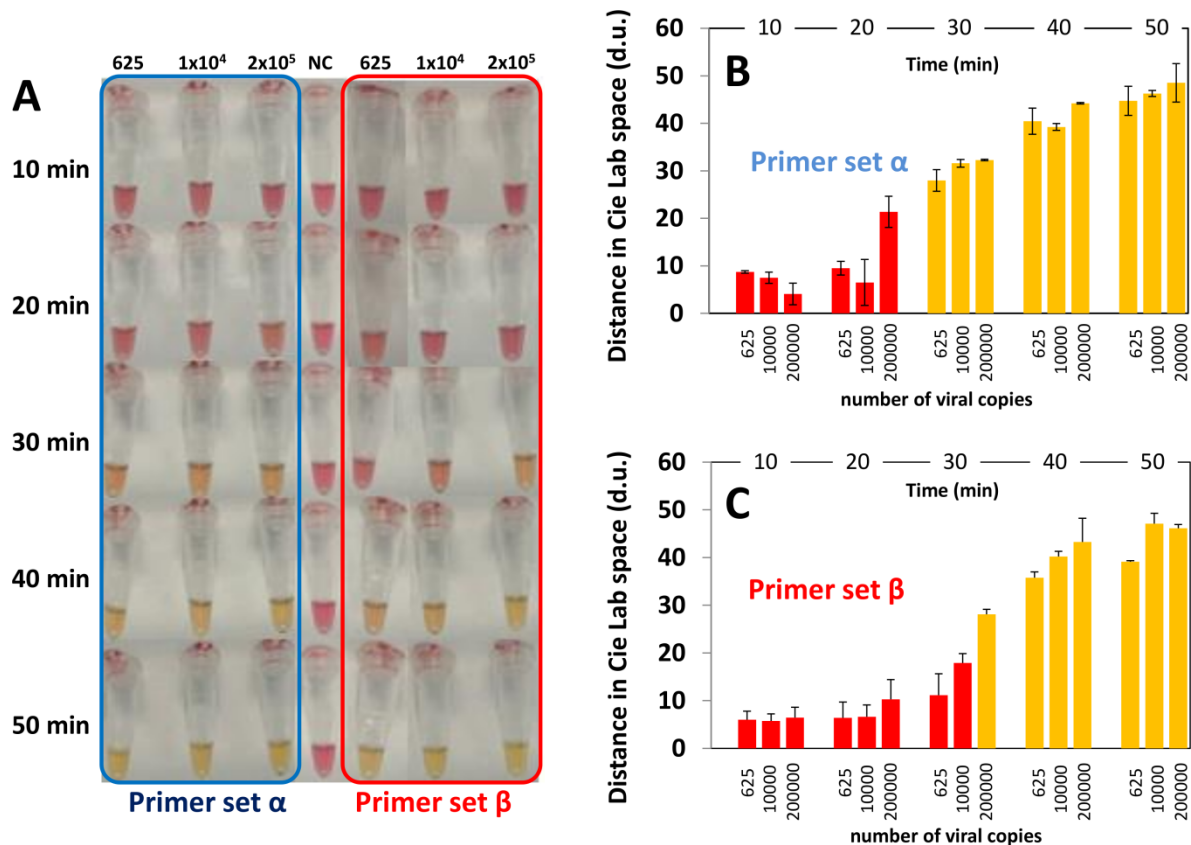
### 253 **Feasibility of real-time quantification**

254 Here, we further illustrate the deterministic and quantitative dependence between the  
255 concentration of the amplification product and the color signal produced during this  
256 colorimetric LAMP reaction. For this purpose, we simulated real-time amplification  
257 experiments by conducting a series of amplification reactions using initial amounts of 625,  
258  $1 \times 10^4$ , and  $2 \times 10^5$  copies of synthetic SARS-CoV-2 genetic material in our 3D-printed  
259 incubator.

260 We extracted samples from the incubator after 0, 10, 20, 30, 40, and 50 min of incubation at  
261 65 °C. The color of these samples was documented as images captured using a smart phone  
262 (iPhone 7) against a white background (Figure 4A). The images were analyzed using the  
263 free access application Color Companion<sup>®</sup> for the iPhone or iPad. Briefly, color images  
264 were decomposed into their CIELab space components. In the CIELab color space, each  
265 color can be represented as a point in a 3D-space, defined by the values **L**, **a**, and **b** [45]. In  
266 this coordinate system, **L** is the luminosity (which ranges from 0 to +100), **a** is the blue-  
267 yellow axis (which ranges from -50 to 50), and **b** is the green-red axis (which ranges from -  
268 50 to 50) (Figure S4).

269 The difference between two colors can be quantitatively represented as the distance  
270 between the two points that those colors represent in the CIELab coordinate system. For the

271 colorimetric LAMP reaction mixture used in our experiments, the spectrum of possible  
272 colors evolves from red (for negative controls and negative samples) to yellow (for positive  
273 samples). Conveniently, the full range of colors for samples and controls can be represented  
274 in the red and yellow quadrant defined by L [0,50], a [0,50], and b [0,50]. For instance, the  
275 difference between the color of a sample (at any time of the reaction) and the color of the  
276 negative control (red;  $L=53.72 \pm 0.581$ ,  $a=38.86 \pm 2.916$ , and  $b=11.86 \pm 0.961$ ) can be  
277 calculated in the CIE Lab space. We determined the distance in the CIE Lab space between  
278 the color of samples taken at different incubation times that contained SARS-CoV-2  
279 genetic material and negative controls (Figure 4B, C). We repeated this calculation for each  
280 of the LAMP primer sets that we used, namely primer set  $\alpha$  (Figure 4B) and  $\beta$  (Figure 4C).



281

282 **Figure 4.** Evaluation of the sensitivity of the combined use of a colorimetric LAMP method  
283 assisted by the use of phenol red. (A) Sensitivity trials using different concentrations of the template

284 (positive control) and two different primers sets:  $\alpha$  (indicated in blue) and  $\beta$  (indicated in red).  
285 Photographs of the Eppendorf PCR tubes containing positive samples and negative controls were  
286 acquired using a smartphone. (C, D) Distance in the color CIELab space between negative controls  
287 (red) and samples containing different concentrations of SARS-CoV-2 nucleic acid material (i.e.,  
288 625, 10000, and 200000 synthetic copies) analyzed after different times of incubation (i.e., 10, 20,  
289 30, 40, and 50 minutes) at 65 °C. The analysis of color distances is presented for amplifications  
290 conducted using primer set (B)  $\alpha$  and (C)  $\beta$ .

291

292

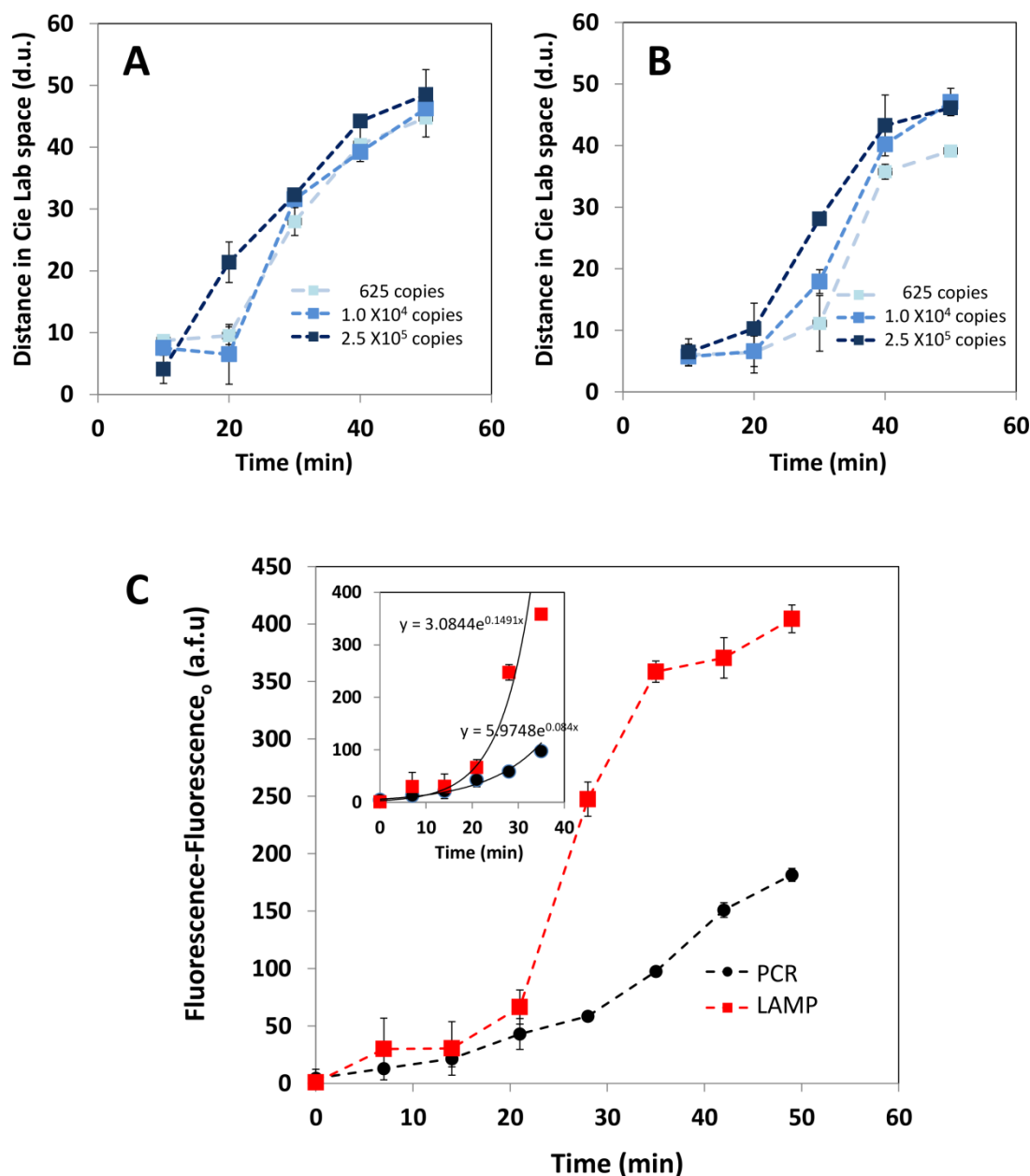
293 These results suggest that the color difference between the samples and negative controls is  
294 quantifiable. Therefore, color analysis may be implemented to assist the discrimination  
295 between positives and negatives. Furthermore, imaging and color analysis techniques may  
296 be implemented in this simple colorimetric LAMP diagnostic strategy to render a real-time  
297 quantitative Lamp (RT-qLAMP). Alternatively, the progression of the amplification at  
298 different times can be monitored by adding an intercalating DNA agent (i.e., EvaGreen  
299 Dye), and measuring fluorescence on time (Figure S5).

300 Note that the variance coefficients for the control are 1.08, 7.50, and 8.10% for L, a, and b,  
301 respectively. These small values suggest robustness and reproducibility in the location of  
302 the coordinates of the control point (reference point). Similarly, the variation in color  
303 between negative controls and positive samples incubated for 50 min was reproducible and  
304 robust (average of 46.60 +/- 4.02 d.u.; variance coefficient of 8.62%).

305 Interestingly, we observed significant differences in the performance of the two LAMP  
306 primer sets used in the experiments reported here (Figures 4B and 5).

307 Our results suggest that primer set  $\alpha$  enabled faster amplification in samples with fewer  
308 viral copies. Consistently, this primer set yielded positive discrimination in samples with

309 625 viral copies in 30 min (Figure 4B). The use of primer set  $\beta$  enabled similar differences  
310 in color, measured as distances in the CIELAB 3D-space, in 40 min (Figure 4C).



311

312 **Figure 5.** Time progression of the distance in color with respect to negative controls (red color) in  
313 the CIELab space for positive SARS-CoV-2 samples containing 625 (light blue,  $\blacksquare$ ),  $1 \times 10^4$   
314 (medium blue,  $\blacksquare$ ), and  $2.5 \times 10^6$  (dark blue,  $\blacksquare$ ) copies of synthetic of SARS-CoV-2 nucleic acids.  
315 Results obtained in experiments using (A) primer set  $\alpha$ , and (B) primer set  $\beta$ . (C) Comparison  
316 between the performance of PCR and LAMP in a simulated real-time experiment. Progression of



317 the fluorescence signal, as measured in a plate reader, in PCR (black circles) and LAMP (red  
318 squares) experiments. The inset shows a zoom at the exponential stage of the amplification process.  
319

320 These findings suggest that primer set  $\alpha$  should be preferred for final-point implementations  
321 of this colorimetric LAMP method. Interestingly, primer set  $\beta$  may better serve the purpose  
322 of a real-time implementation. While primer set  $\alpha$  produced similar trajectories of evolution  
323 of color in samples that contained  $1.0 \times 10^4$  and  $2.0 \times 10^5$  viral copies (Figure 5A), primer  
324 set  $\beta$  was better at discriminating between amplifications produced from different initial  
325 viral loads (Figure 5B).

326

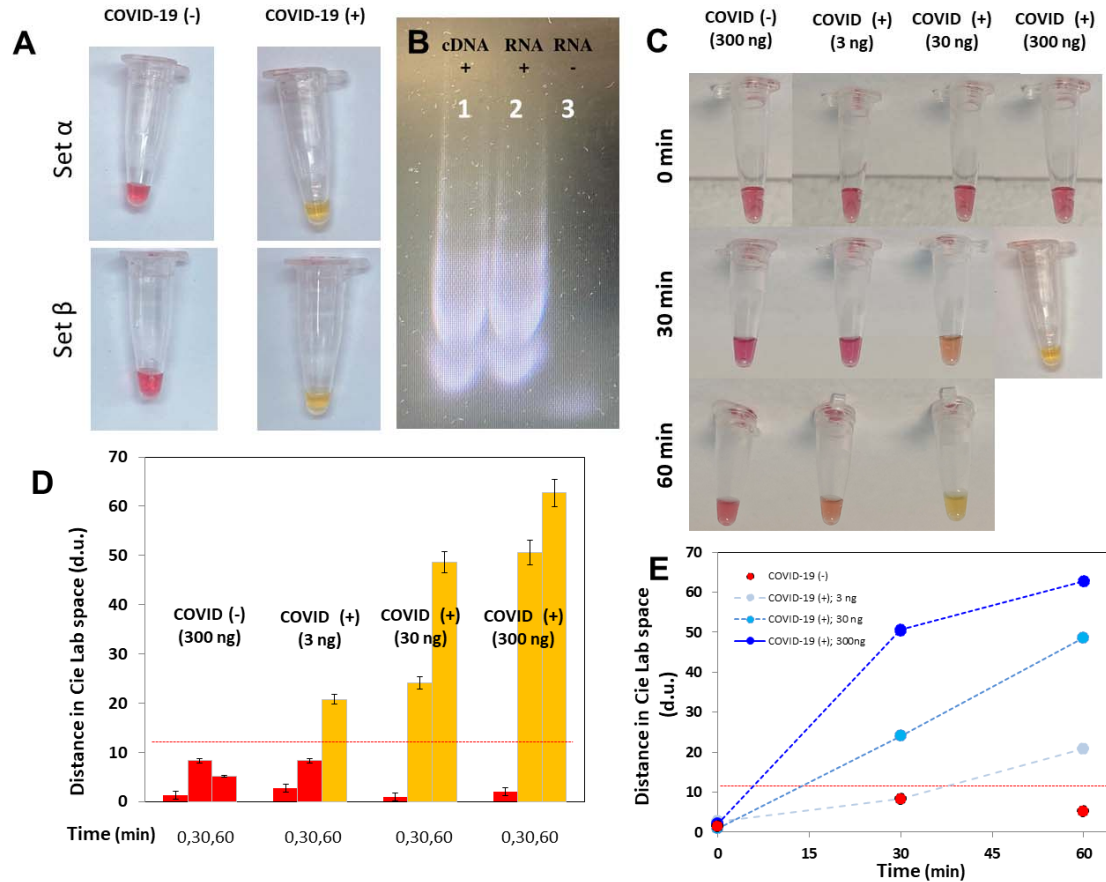
### 327 **Comparison of LAMP versus PCR**

328 LAMP has been regarded before as a more efficient amplification reaction than PCR, since  
329 more DNA is produced per unit of time due to the use of a higher number of primers[50]  
330 (in this case 6 versus 2). To finalize our analysis, we simulated some real-time  
331 amplification experiments to compare the performance of LAMP and PCR in similar  
332 conditions (Figure 6A). To that end, we conducted amplification reactions using initial  
333 amounts of  $4 \times 10^4$  copies of synthetic SARS-CoV2 in a commercial miniPCR  
334 cycler[24,51] (using primer set N1) and in our LAMP 3D-printed incubator (using primer  
335 set  $\beta$ ). We added the intercalating agent, EvaGreen<sup>®</sup> Dye, to the reaction mix at the initial  
336 time and extracted samples after 0, 7, 14, 21, 28, 35, 42, and 51 minutes. These samples  
337 from PCR and LAMP experiments were dispensed in 96-well plates. The fluorescence  
338 from these samples was then measured in a commercial plate reader[24] (Figure 5C). We  
339 observed an exponential increase in fluorescence as more LAMP or PCR cycles were  
340 performed, which highlights the quantitative nature of the intercalating reaction. The  
341 LAMP reaction produces significantly higher fluorescence signals than the PCR reaction

342 throughout the entire reaction time. The difference between the fluorescence emissions of  
343 both amplifications is more evident after the first 20 minutes of amplification. These  
344 results also suggest that using a commercial plate reader to determine the extent of advance  
345 of LAMP amplifications is a practical and reliable alternative to the use of colorimetric  
346 evaluations. Moreover, fluorescence reading of LAMP products may lead to precise  
347 quantification of SARS-CoV-2 viral loads.

348 Finally, we compared the performance of RT-qPCR and colorimetric LAMP using actual  
349 RNA extracts isolated from human volunteers. For this purpose, we used colorimetric  
350 LAMP for diagnosis of one RNA sample confirmed as positive for COVID-19 and one  
351 confirmed as negative according to RT-qPCR results. RNA extracts from the COVID-19  
352 (+) patient were clearly discriminated from the COVID-19 (-) patient extracts by our  
353 colorimetric LAMP amplifications (Figure 6A).

354 Similar results were obtained regardless of the LAMP primer set used (i.e.,  $\alpha$  and  $\beta$ ). We  
355 corroborated our LAMP amplification results using standard gel electrophoresis (Figure  
356 6B). In addition, samples were serially diluted to challenge the sensitivity of colorimetric  
357 LAMP. We were able to discriminate between positive and negative samples in the entire  
358 concentration range tested (300 ng of total RNA, as determined by nanoDrop assays). The  
359 color shift (red to yellow) was clearly perceived after 30 minutes of amplification in  
360 samples containing 300 ng of total RNA from COVID (+) patients. Samples containing 30  
361 and 3 ng of total RNA required longer times (Figure 6C). All positive samples exhibited a  
362 shift in color after 60 minutes of amplification, while negative samples remained  
363 unchanged. We quantified the change in color in positive and negative samples using color  
364 image analysis and by calculating color distances in the CieLab color space (Figure 6D,E).



365

366 **Figure 6.** Diagnostics of actual RNA extracts from patients. (A) RNA extracts from COVID-19(+)   
 367 and COVID-19(-) samples, amplified by colorimetric LAMP, can be easily discriminated by visual   
 368 inspection. (B) LAMP amplification products from cDNA (lane 1) and RNA extracts (lane 2) from   
 369 COVID (+) patients, and COVID (-) volunteers (lane 3), as revealed by gel electrophoresis   
 370 experiments. (C) Time progression of color changes in LAMP reaction mixes containing 300 ng of   
 371 RNA extract from a COVID(-) volunteer (as diagnosed by RT-qPCR), and 3, 30, and 300 ng of   
 372 RNA extract from a COVID(+) patient (as diagnosed by RT-qPCR). (D) Distance in color with   
 373 respect to negative controls (red color) in the CieLab space for RNA extracts from a COVID(-)   
 374 volunteer (as diagnosed by RT-qPCR) containing 300 ng of nucleic acids, and a COVID(+) patient   
 375 (as diagnosed by RT-qPCR) containing 3, 30, and 35 (dark blue, ■) ng of nucleic acids. Readings at   
 376 0, 30, and 60 minutes are shown. A suggested positive–negative threshold value is indicated with a   
 377 red line. (E) Time progression of the distance in color with respect to negative controls (red color)   
 378 in the CieLab space for RNA extracts from a COVID(-) volunteer (as diagnosed by RT-qPCR)   
 379 containing 300 ng of nucleic acids (red, ■), and from a COVID(+) patient (as diagnosed by RT-

380 qPCR) containing 3 (light blue, ■), 30 (medium blue, ■), and 35 (dark blue, ■) ng of nucleic acids.

381 A suggested positive–negative threshold value is indicated with a red line.

382

383 Our experiments show that the distance in color between positive and negative RNA

384 samples from human volunteers is proportional to the number of viral copies. These results

385 suggest that the change in color can be quantitatively related to the viral load of SARS-

386 CoV-2 in actual RNA extracts, similarly to synthetic samples.

387 The challenge of point-of-care detection of viral threats is of paramount importance,

388 particularly in underdeveloped regions and in emergency situations (i.e., epidemic

389 outbreaks). In the context of the current COVID-19 pandemic, the availability of testing

390 infrastructure based on RT-qPCR is recognized as a serious challenge around the world. In

391 developing economies (i.e. Latin America, India, and most African countries), the currently

392 available resources for massive COVID-19 testing by RT-qPCR will clearly be insufficient.

393 Even in developed countries, the time to get diagnostic RT-qPCR results from a COVID-19

394 RT-qPCR test currently ranges from 1 to 5 days. Clearly, the available PCR labs are

395 overburdened with samples, have too few personnel to conduct the tests, are struggling with

396 backlogs on the instrumentation, and face complicated logistics to transport delicate and

397 infective samples while preserving the cold chain.

398 Here, we have demonstrated that a simple embodiment of a LAMP reaction, assisted by the

399 use of phenol red as a pH indicator and the use of a simple 3D-printed chamber connected

400 to a water circulator, can enable the rapid and highly accurate identification of samples that

401 contain artificial SARS-CoV-2 genetic sequences. Amplification is visually evident,

402 without the need for any additional instrumentation, even at low viral copy numbers. In our

403 experiments with synthetic samples, we observed 100% accuracy in samples containing as  
404 few as 625 copies of SARS-CoV-2 genetic material.

405 Validation of these results using a larger number of real human samples from positive and  
406 negative COVID-19 subjects is obviously needed to obtain a full assessment of the  
407 potential of this strategy as an alternative to RT-qPCR platforms. However, our results with  
408 synthetic samples and with a reduced number of samples containing RNA from human  
409 volunteers suggest that this simple strategy may greatly enhance the capabilities for  
410 COVID-19 testing in situations where RT-qPCR is not feasible or is unavailable.

411

## 412 **Materials and Methods**

413 *Equipment specifications:* We ran several hundred amplification experiments using a  
414 colorimetric LAMP method in a 3D-printed incubation chamber designed in house and  
415 connected to a conventional water circulator (Figure 1). The design and all dimensional  
416 specifications of this chamber have been made available in Supplementary Information  
417 (Figures S1, S2; Supplementary File S1). In the experiments reported here, we used a  
418 chamber with dimensions of  $20 \times 5 \times 15 \text{ cm}^3$  and a weight of 0.4 kg (without water). A  
419 conventional water circulator (WVR, PA, USA), was used to circulate hot water (set point  
420 value at 76 °C) through the 3D-printed chamber for incubation of the Eppendorf PCR tubes  
421 (0.2 mL). In this first chamber prototype, twelve amplification reactions can be run in  
422 parallel. This concept design is amenable for fabrication in any STL-3D printing platform  
423 and may be scaled up to accommodate a larger number of tubes.

424 We used a blueGel electrophoresis unit, powered by 120 AC volts, to validate the LAMP  
425 amplification using gel electrophoresis. Photo-documentation was done using a

426 smartphone camera. We also used a Synergy HT microplate reader (BioTek Instruments,  
427 VT, USA) to detect the fluorescence induced by an intercalating reagent in positive  
428 samples from the PCR reactions.

429 *Validation DNA templates:* We used plasmids containing the complete N gene from 2019-  
430 nCoV, SARS, and MERS as positive controls, with a concentration of 200,000 copies/ $\mu$ L  
431 (Integrated DNA Technologies, IA, USA). Samples containing different concentrations of  
432 synthetic nucleic acids of SARS-CoV-2 were prepared by successive dilutions from stocks  
433 (from  $2 \times 10^5$  copies to 65 copies). We used a plasmid that contained the gene GP from  
434 EBOV as a negative control. The production of this EBOV genetic material has been  
435 documented elsewhere by our group [23].

436 *RNA extracts from human volunteers.* In addition, we used two samples of RNA extracts  
437 from COVID-19 positive and negative subjects, as determined by RT-PCR analysis.  
438 Samples were kindly donated by Hospital Alfa, Medical Center, in Guadalupe, Nuevo  
439 León, México. Nasopharyngeal samples were collected from two patients after obtaining  
440 informed and signed written consent and in complete observance of good clinical practices,  
441 the principles stated in the Helsinki Declaration, and applicable lab operating procedures at  
442 Hospital Alfa. Every precaution was taken to protect the privacy of sample donors and the  
443 confidentiality of their personal information. RNA extraction and purification was  
444 conducted at the molecular biology laboratory at Hospital Alfa. The Qiagen QIAamp DSP  
445 Viral RNA Mini kit was used for RNA extraction and purification by closely following the  
446 directions of the manufacturer.

447 *Amplification mix:* We used WarmStart<sup>®</sup> Colorimetric LAMP 2× Master Mix (DNA &  
448 RNA) from New England Biolabs (MA, USA), and followed the recommended protocol:  
449 12.5 μL Readymix, 1.6 μM FIP primer, 1.6 μM BIP primer, 0.2 μM F3 primer, 0.2 μM B3  
450 primer, 0.4 μM LF primer, 0.4 μM LB primer, 1 μL DNA template (~ 625 to  $2 \times 10^5$  DNA  
451 copies), 1.25 μL EvaGreen<sup>®</sup> Dye from Biotium (CA, USA), and nuclease-free water to a  
452 final volume of reaction 25 μL. This commercial mix contains phenol red as a pH indicator  
453 for revealing the shift of pH during LAMP amplification across the threshold of pH=6.8.

454

455 *Primers used:* Two different sets of LAMP primers, referred to here as  $\alpha$  and  $\beta$ , were  
456 designed in house using the LAMP primer design software Primer Explorer V5  
457 (<http://primerexplorer.jp/lampv5e/index.html>). These primers were based on the analysis of  
458 alignments of the SARS-Co2 N gene sequences using the software Geneious (Auckland,  
459 New Zealand), downloaded from [https://www.ncbi.nlm.nih.gov/genbank/sars-cov-2-](https://www.ncbi.nlm.nih.gov/genbank/sars-cov-2-seqs/#nucleotide-sequences)  
460 [seqs/#nucleotide-sequences](https://www.ncbi.nlm.nih.gov/genbank/sars-cov-2-seqs/#nucleotide-sequences).

461 Each set, containing six LAMP primers, were used to target two different regions of the  
462 sequence of the SARS-Co2 N gene. In addition, for comparison purposes, we conducted  
463 PCR amplification experiments using one of the primer sets recommended by the CDC for  
464 the standard diagnostics of COVID-19 (i.e., N1 assay) using RT-qPCR. The sequences of  
465 our LAMP primers are presented in Table 1. The sequences of the PCR primers (N1) have  
466 been reported elsewhere[24,46].

467

468 *Amplification protocols:* For all LAMP experiments, we performed isothermal heating for  
469 30 or 60 min. In our experiments, we tested three different temperatures: 50, 60, and 65 °C.

470 For PCR experiments, we used a three-stage protocol consisting of a denaturation stage at  
471 94 °C for 5 min, followed by 25 cycles of 94 °C for 20 s, 60 °C for 30 s, and 72 °C for 20  
472 s, and then a final stage at 72 °C for 5 min, for a total duration of 60 min in the miniPCR®  
473 thermocycler from Amplyus (MA, USA).

474

475 *Documentation of LAMP products:* We analyzed 10 µL of each LAMP reaction in a  
476 blueGel unit, a portable electrophoresis unit sold by MiniPCR from Amplyus (MA, USA).  
477 This is a compact electrophoresis unit (23 × 10 × 7 cm<sup>3</sup>) that weighs 350 g. In these  
478 experiments, we analyzed 10 µL of the LAMP product using 1.2% agarose electrophoresis  
479 tris-borate-EDTA buffer (TBE). We used the Quick-Load Purple 2-Log DNA Ladder  
480 (NEB, MA, USA) as a molecular weight marker. Gels were dyed with Gel-Green from  
481 Biotium (CA, USA) using a 1:10,000 dilution, and a current of 48 V was supplied by the  
482 blueGel built-in power supply (AC 100–240V, 50–60Hz).

483 As an alternative method for detection and reading of the amplification product, we  
484 evaluated the amplification products by detecting the fluorescence emitted by a DNA-  
485 intercalating agent, the EvaGreen® Dye from Biotium (CA, USA), in a Synergy HT  
486 microplate reader (BioTek Instruments, VT, USA). Briefly, 25 µL of the LAMP reaction  
487 was placed in separate wells of a 96-well plate following completion of the LAMP  
488 incubation. A 125 µL volume of nuclease-free water was added to each well for a final  
489 sample volume of 150 µL and the samples were well-mixed by pipetting. These  
490 experiments were run in triplicate. The following conditions were used in the microplate  
491 reader: excitation of 485/20, emission of 528/20, gain of 75. Fluorescence readings were  
492 done from the top at room temperature.

493



494 *Color determination by image analysis:* We also photographically documented and  
495 analyzed the progression of color changes in the positive and negative SARS-CoV-2  
496 synthetic samples during the LAMP reaction time (i.e., from 0 to 50 min). For that purpose,  
497 Eppendorf PCR tubes containing LAMP samples were photographed using a smartphone  
498 (iPhone, from Apple, USA). We used an application for IOS (Color Companion, freely  
499 available at Apple store) to determine the components of color of each LAMP sample in the  
500 CIELab color space. Color differences between the positive samples and negative controls  
501 were calculated as distances in the CIELab coordinate system according to the following  
502 formula:

$$504 \text{ Color Distance}_{\text{sample-negative}} = \text{SQRT} [(L_{\text{sample}} - L_{\text{negative}})^2 + (a_{\text{sample}} - a_{\text{negative}})^2 + (b_{\text{sample}} - b_{\text{negative}})^2]$$

505  
506 Here L, a, and b are the color components of the sample or the negative control in the  
507 CIELab color space (Figure S4).

## 509 **Acknowledgments**

510 The authors acknowledge the funding provided by the Federico Baur Endowed Chair in  
511 Nanotechnology (0020240I03). EGG acknowledges funding from a doctoral scholarship  
512 provided by CONACyT (Consejo Nacional de Ciencia y Tecnología, México). GTdS and  
513 MMA acknowledge the institutional funding received from Tecnológico de Monterrey  
514 (Grant 002EICIS01). MMA, GTdS, SOMC and IMLM acknowledge funding provided by  
515 CONACyT (Consejo Nacional de Ciencia y Tecnología, México) through grants SNI

516 26048, SNI 256730, SNI 31803, SNI 1056909, respectively. YSZ acknowledges the support  
517 by the Brigham Research Institute.

518

## 519 **Supporting Information**

520 **Figure S1.** (A) Photograph and (B) rendering of the 3D-printed incubation chamber used in  
521 LAMP experiments.

522 **Figure S2.** Schematic representation of the chamber (different views) showing its relevant  
523 dimensions.

524 **Figure S3.** Commercial plasmid that contains the plasmids containing the complete N gene  
525 from 2019-nCoV, SARS, and MERS. We use this plasmid as a SARS-CoV-2 synthetic  
526 nucleic acid material in our amplification experiments

527 **Figure S4.** *In house* designed plasmid containing the gene that codes for the expression of  
528 protein GP from EBOV. This plasmid was added as nucleic acid material in negative  
529 controls in our amplification experiments

530 **Figure S5.** (A) The colorimetric LAMP method described here was able to identify and  
531 amplify synthetic SARS-CoV-2 genetic material in samples containing as few as ~62 viral  
532 copies. (B) Evaluation of the stability and functionality of the LAMP reaction mix at  
533 different storage times and temperatures. The reaction mix, which is formulated with  
534 LAMP primers and ready for the addition of nucleic acid extracts, is functional and  
535 discriminates between positive and negative samples when stored (i) at room temperature  
536 for 48 h or (ii) at 4 °C for 72 h.

537 **Figure S6.** (A) Color analysis conducted on positive and negative SARS-CoV-2 samples  
538 contained in Eppendorf PCR tubes (yellow inset) using Color Companion, a freely  
539 available app from Apple (downloadable at Apple Store, USA). This app identifies the  
540 components of color in a specific location of an image (black circle in the yellow inset) in  
541 the CIELab, RGB, HSB, or CMYK spaces. The image can be uploaded using e-mail,  
542 airdrop, or Whatsapp. (B) Schematic representation of the CIELab space, a color system  
543 where any color can be represented in terms of a point and its coordinates in a 3D space,  
544 where L is luminosity, a is the axis between green and red, and b is the axis between yellow  
545 and red.

546 **Figure S7.** (A) The amount of amplification product in LAMP experiments was evaluated  
547 by measuring the fluorescence emitted by the amplification product in reactions with an  
548 added intercalating agent. Fluorescence readings were conducted in standard 96-well plates  
549 using a conventional plate reader. (A) Fluorescence readings, as measured in a commercial  
550 plate reader, for different dilutions of SARS-CoV-2 synthetic DNA templates. Results  
551 using two different LAMP primer sets are shown: set  $\alpha$  (indicated in blue), and set  $\beta$   
552 (indicated in red).

553

## 554 **References**

- 555 1. Coronavirus Disease (COVID-19) – Statistics and Research - Our World in Data  
556 [Internet]. [cited 8 Apr 2020]. Available:  
557 [https://ourworldindata.org/coronavirus?fbclid=IwAR28tcRVA1rmXsVCrYHcxuHp](https://ourworldindata.org/coronavirus?fbclid=IwAR28tcRVA1rmXsVCrYHcxuHpRXeyO9-uxFJFSG5-lv5gsJgzDxK7eN08i_Y)  
558 [RXeyO9-uxFJFSG5-lv5gsJgzDxK7eN08i\\_Y](https://ourworldindata.org/coronavirus?fbclid=IwAR28tcRVA1rmXsVCrYHcxuHpRXeyO9-uxFJFSG5-lv5gsJgzDxK7eN08i_Y)
- 559 2. Bedford J, Enria D, Giesecke J, Heymann DL, Ihekweazu C, Kobinger G, et al.  
560 COVID-19: towards controlling of a pandemic. *The Lancet*. Lancet Publishing  
561 Group; 2020. pp. 1015–1018. doi:10.1016/S0140-6736(20)30673-5
- 562 3. Cohen J, Kupferschmidt K. Countries test tactics in “war” against COVID-19.  
563 *Science*. American Association for the Advancement of Science; 2020;367: 1287–  
564 1288. doi:10.1126/science.367.6484.1287
- 565 4. Pung R, Chiew CJ, Young BE, Chin S, I-C Chen M, Clapham HE, et al. Articles  
566 Investigation of three clusters of COVID-19 in Singapore: implications for  
567 surveillance and response measures. *Lancet*. Elsevier; 2020;19: 1–8.  
568 doi:10.1016/S0140-6736(20)30528-6
- 569 5. Alvarez MM, Gonzalez-Gonzalez E, Santiago GT. Modeling COVID-19 epidemics  
570 in an Excel spreadsheet: Democratizing the access to first-hand accurate predictions  
571 of epidemic outbreaks. medRxiv. Cold Spring Harbor Laboratory Press; 2020;

- 572 2020.03.23.20041590. doi:10.1101/2020.03.23.20041590
- 573 6. Singh R, Adhikari R. Age-structured impact of social distancing on the COVID-19  
574 epidemic in India. 2020; Available: <http://arxiv.org/abs/2003.12055>
- 575 7. Bastos SB, Cajueiro DO. Modeling and forecasting the Covid-19 pandemic in  
576 Brazil. 2020; Available: <http://arxiv.org/abs/2003.14288>
- 577 8. Yen C-W, de Puig H, Tam JO, Gómez-Márquez J, Bosch I, Hamad-Schifferli K, et  
578 al. Multicolored silver nanoparticles for multiplexed disease diagnostics:  
579 distinguishing dengue, yellow fever, and Ebola viruses. *Lab Chip. The Royal Society*  
580 *of Chemistry*; 2015;15: 1638–1641. doi:10.1039/C5LC00055F
- 581 9. Mou L, Jiang X. Materials for Microfluidic Immunoassays: A Review. *Adv Healthc*  
582 *Mater. Wiley-VCH Verlag*; 2017;6: 1601403. doi:10.1002/adhm.201601403
- 583 10. Alvarez MM, López-Pacheco F, Aguilar-Yañez JM, Portillo-Lara R, Mendoza-  
584 Ochoa GI, García-Echauri S, et al. Specific Recognition of Influenza A/H1N1/2009  
585 Antibodies in Human Serum: A Simple Virus-Free ELISA Method. Jeyaseelan S,  
586 editor. *PLoS One. Public Library of Science*; 2010;5: e10176.  
587 doi:10.1371/journal.pone.0010176
- 588 11. Zhong L, Chuan J, Gong B, Shuai P, Zhou Y, Zhang Y, et al. Detection of serum  
589 IgM and IgG for COVID-19 diagnosis. *Sci CHINA Life Sci. Science China Press*;  
590 2020; doi:10.1007/S11427-020-1688-9
- 591 12. Pardee K, Green AA, Takahashi MK, Braff D, Lambert G, Lee JW, et al. Rapid,  
592 Low-Cost Detection of Zika Virus Using Programmable Biomolecular Components.  
593 *Cell. Cell Press*; 2016;165: 1255–1266. doi:10.1016/J.CELL.2016.04.059
- 594 13. Broughton JP, Deng X, Yu G, Fasching CL, Streithorst J, Granados A, et al. Rapid  
595 Detection of 2019 Novel Coronavirus SARS-CoV-2 Using a CRISPR-based 1

- 596 DETECTR Lateral Flow Assay 2 3. doi:10.1101/2020.03.06.20032334
- 597 14. Chen JS, Ma E, Harrington LB, Da Costa M, Tian X, Palefsky JM, et al. CRISPR-  
598 Cas12a target binding unleashes indiscriminate single-stranded DNase activity.  
599 Science (80- ). American Association for the Advancement of Science; 2018;360:  
600 436–439. doi:10.1126/science.aar6245
- 601 15. Elizondo-Montemayor L, Alvarez MM, Hernández-Torre M, Ugalde-Casas PA,  
602 Lam-Franco L, Bustamante-Careaga H, et al. Seroprevalence of antibodies to  
603 influenza A/H1N1/2009 among transmission risk groups after the second wave in  
604 Mexico, by a virus-free ELISA method. *Int J Infect Dis. Elsevier*; 2011;15: e781–  
605 e786. doi:10.1016/j.ijid.2011.07.002
- 606 16. Tang Y-W, Schmitz JE, Persing DH, Stratton CW. The Laboratory Diagnosis of  
607 COVID-19 Infection: Current Issues and Challenges. *J Clin Microbiol. American  
608 Society for Microbiology Journals*; 2020; doi:10.1128/JCM.00512-20
- 609 17. Wölfel R, Corman VM, Guggemos W, Seilmaier M, Zange S, Müller MA, et al.  
610 Virological assessment of hospitalized patients with COVID-2019. *Nature. Nature  
611 Publishing Group*; 2020; 1–10. doi:10.1038/s41586-020-2196-x
- 612 18. Mauk MG, Song J, Bau HH, Liu C. Point-of-Care Molecular Test for Zika Infection.  
613 *Clin Lab Int. NIH Public Access*; 2017;41: 25–27. Available:  
614 <http://www.ncbi.nlm.nih.gov/pubmed/28819345>
- 615 19. Liao S-C, Peng J, Mauk MG, Awasthi S, Song J, Friedman H, et al. Smart cup: A  
616 minimally-instrumented, smartphone-based point-of-care molecular diagnostic  
617 device. *Sensors Actuators B Chem. Elsevier*; 2016;229: 232–238.  
618 doi:10.1016/J.SNB.2016.01.073
- 619 20. Jansen van Vuren P, Grobbelaar A, Storm N, Conteh O, Konneh K, Kamara A, et al.

- 620 Comparative Evaluation of the Diagnostic Performance of the Prototype Cepheid  
621 GeneXpert Ebola Assay. *J Clin Microbiol. American Society for Microbiology*;  
622 2016;54: 359–67. doi:10.1128/JCM.02724-15
- 623 21. Craw P, Balachandran W. Isothermal nucleic acid amplification technologies for  
624 point-of-care diagnostics: a critical review. *Lab Chip. The Royal Society of*  
625 *Chemistry*; 2012;12: 2469. doi:10.1039/c2lc40100b
- 626 22. Hsieh K, Patterson AS, Ferguson BS, Plaxco KW, Soh HT. Rapid, sensitive, and  
627 quantitative detection of pathogenic DNA at the point of care through microfluidic  
628 electrochemical quantitative loop-mediated isothermal amplification. *Angew Chem*  
629 *Int Ed Engl. NIH Public Access*; 2012;51: 4896–900. doi:10.1002/anie.201109115
- 630 23. Gonzá Lez-Gonzá Lez E, Mendoza-Ramos JL, Pedrozaid SC, Cuellar-Monterrubbio  
631 A, Má Rquez-Ipiña AR, Lira-Serhanid D, et al. Validation of use of the miniPCR  
632 thermocycler for Ebola and Zika virus detection. 2019;  
633 doi:10.1371/journal.pone.0215642
- 634 24. Gonzalez-Gonzalez E, Santiago GT, Lara-Mayorga IM, Martinez-Chapa SO,  
635 Alvarez MM. Portable and accurate diagnostics for COVID-19: Combined use of the  
636 miniPCR thermocycler and a well-plate reader for SARS-Co2 virus detection.  
637 medRxiv. Cold Spring Harbor Laboratory Press; 2020; 2020.04.03.20052860.  
638 doi:10.1101/2020.04.03.20052860
- 639 25. Lan L, Xu D, Ye G, Xia C, Wang S, Li Y, et al. Positive RT-PCR Test Results in  
640 Patients Recovered From COVID-19. *JAMA*. 2020; doi:10.1001/jama.2020.2783
- 641 26. El-Tholoth M, Bau HH, Song J. A Single and Two-Stage, Closed-Tube, Molecular  
642 Test for the 2019 Novel Coronavirus (COVID-19) at Home, Clinic, and Points of  
643 Entry. *ChemRxiv*; 2020; doi:10.26434/CHEMRXIV.11860137.V1

- 644 27. Kaarj K, Akarapipad P, Yoon JY. Simpler, Faster, and Sensitive Zika Virus Assay  
645 Using Smartphone Detection of Loop-mediated Isothermal Amplification on Paper  
646 Microfluidic Chips. *Sci Rep. Nature Publishing Group*; 2018;8: 1–11.  
647 doi:10.1038/s41598-018-30797-9
- 648 28. Tomita N, Mori Y, Kanda H, Notomi T. Loop-mediated isothermal amplification  
649 (LAMP) of gene sequences and simple visual detection of products. *Nat Protoc.*  
650 *Nature Publishing Group*; 2008;3: 877–882. doi:10.1038/nprot.2008.57
- 651 29. Goto M, Honda E, Ogura A, Nomoto A, Hanaki KI. Colorimetric detection of loop-  
652 mediated isothermal amplification reaction by using hydroxy naphthol blue.  
653 *Biotechniques.* 2009;46: 167–172. doi:10.2144/000113072
- 654 30. Yang T, Wang Y-C, Shen C-F, Cheng C-M. Point-of-Care RNA-Based Diagnostic  
655 Device for COVID-19. *Diagnostics. MDPI AG*; 2020;10: 165.  
656 doi:10.3390/diagnostics10030165
- 657 31. Kozel TR, Burnham-Marusich AR. Point-of-Care Testing for Infectious Diseases:  
658 Past, Present, and Future. *J Clin Microbiol. American Society for Microbiology*;  
659 2017;55: 2313–2320. doi:10.1128/JCM.00476-17
- 660 32. Su W, Gao X, Jiang L, Qin J. Microfluidic platform towards point-of-care  
661 diagnostics in infectious diseases. *J Chromatogr A. Elsevier*; 2015;1377: 13–26.  
662 doi:10.1016/J.CHROMA.2014.12.041
- 663 33. Drancourt M, Michel-Lepage A, Boyer S, Raoult D. The Point-of-Care Laboratory  
664 in Clinical Microbiology. *Clin Microbiol Rev. American Society for Microbiology*;  
665 2016;29: 429–47. doi:10.1128/CMR.00090-15
- 666 34. Jangam SR, Agarwal AK, Sur K, Kelso DM. A point-of-care PCR test for HIV-1  
667 detection in resource-limited settings. *Biosens Bioelectron. Elsevier*; 2013;42: 69–75.

- 668 doi:10.1016/J.BIOS.2012.10.024
- 669 35. Qiu X, Ge S, Gao P, Li K, Yang S, Zhang S, et al. A smartphone-based point-of-care  
670 diagnosis of H1N1 with microfluidic convection PCR. *Microsyst Technol.* Springer  
671 Berlin Heidelberg; 2017;23: 2951–2956. doi:10.1007/s00542-016-2979-z
- 672 36. Nguyen T, Duong Bang D, Wolff A. 2019 Novel Coronavirus Disease (COVID-19):  
673 Paving the Road for Rapid Detection and Point-of-Care Diagnostics.  
674 *Micromachines.* MDPI AG; 2020;11: 306. doi:10.3390/mi11030306
- 675 37. Udugama B, Kadhiresan P, Kozlowski HN, Malekjahani A, Osborne M, Li VYC, et  
676 al. Diagnosing COVID-19: The Disease and Tools for Detection. *ACS Nano.*  
677 American Chemical Society; 2020; doi:10.1021/acsnano.0c02624
- 678 38. Gates B. Responding to Covid-19 — A Once-in-a-Century Pandemic? *N Engl J*  
679 *Med.* Massachusetts Medical Society; 2020; doi:10.1056/nejmp2003762
- 680 39. Yu L, Wu S, Hao X, Li X, Liu X, Ye S, et al. Rapid colorimetric detection of  
681 COVID-19 coronavirus using a reverse tran-scriptional loop-mediated isothermal  
682 amplification (RT-LAMP) diagnostic plat-form: iLACO. medRxiv. Cold Spring  
683 Harbor Laboratory Press; 2020; 2020.02.20.20025874.  
684 doi:10.1101/2020.02.20.20025874
- 685 40. Zhang Y, Odiwuor N, Xiong J, Sun L, Nyaruaba RO, Wei H, et al. Rapid Molecular  
686 Detection of SARS-CoV-2 (COVID-19) Virus RNA Using Colorimetric LAMP.  
687 medRxiv. Cold Spring Harbor Laboratory Press; 2020;2: 2020.02.26.20028373.  
688 doi:10.1101/2020.02.26.20028373
- 689 41. Park G-S, Ku K, Beak S-H, Kim SJ, Kim S Il, Kim B-T, et al. Development of  
690 Reverse Transcription Loop-mediated Isothermal Amplification (RT-LAMP) Assays  
691 Targeting SARS-CoV-2. bioRxiv. Cold Spring Harbor Laboratory; 2020;

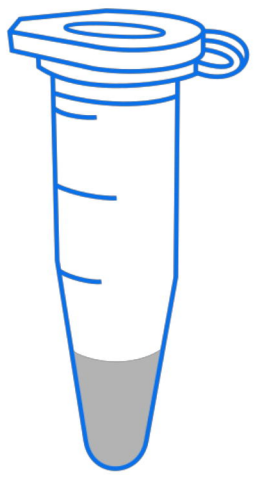


- 692 2020.03.09.983064. doi:10.1101/2020.03.09.983064
- 693 42. Zhu X, Wang X, Han L, Chen T, Wang L, Li H, et al. Reverse transcription loop-  
694 mediated isothermal amplification combined with nanoparticles-based biosensor for  
695 diagnosis of COVID-19. medRxiv. Cold Spring Harbor Laboratory Press; 2020;  
696 2020.03.17.20037796. doi:10.1101/2020.03.17.20037796
- 697 43. Lamb LE, Bartolone SN, Ward E, Chancellor MB. Rapid Detection of Novel  
698 Coronavirus (COVID19) by Reverse Transcription-Loop-Mediated Isothermal  
699 Amplification. SSRN Electron J. Elsevier BV; 2020; doi:10.2139/ssrn.3539654
- 700 44. Jiang M, Fang W, Aratehfar A, Li X, ling L, Fang H, et al. Development and  
701 validation of a rapid single-step reverse transcriptase loop-mediated isothermal  
702 amplification (RT-LAMP) system potentially to be used for reliable and high-  
703 throughput screening of COVID-19. medRxiv. Cold Spring Harbor Laboratory  
704 Press; 2020; 2020.03.15.20036376. doi:10.1101/2020.03.15.20036376
- 705 45. Santiago GT De, Gante CR De, García-Lara S, Ballescá-Estrada A, Alvarez MM.  
706 Studying mixing in Non-Newtonian blue maize flour suspensions using color  
707 analysis. PLoS One. Public Library of Science; 2014;9.  
708 doi:10.1371/journal.pone.0112954
- 709 46. OSF Preprints | Landscape Coronavirus Disease 2019 test (COVID-19 test) in vitro -  
710 - A comparison of PCR vs Immunoassay vs Crispr-Based test [Internet]. [cited 8 Apr  
711 2020]. Available: <https://osf.io/6eagn>
- 712 47. Tanner NA, Zhang Y, Evans TC. Visual detection of isothermal nucleic acid  
713 amplification using pH-sensitive dyes. Biotechniques. Eaton Publishing Company;  
714 2015;58: 59–68. doi:10.2144/000114253
- 715 48. Rusk N. Torrents of sequence. Nature Methods. Nature Publishing Group; 2011. p.

- 716 44. doi:10.1038/nmeth.f.330
- 717 49. Wang W, Xu Y, Gao R, Lu R, Han K, Wu G, et al. Detection of SARS-CoV-2 in  
718 Different Types of Clinical Specimens. *JAMA - Journal of the American Medical*  
719 *Association*. American Medical Association; 2020. doi:10.1001/jama.2020.3786
- 720 50. Gadkar VJ, Goldfarb DM, Gantt S, Tilley PAG. Real-time Detection and Monitoring  
721 of Loop Mediated Amplification (LAMP) Reaction Using Self-quenching and De-  
722 quenching Fluorogenic Probes. *Sci Rep*. Nature Publishing Group; 2018;8: 1–10.  
723 doi:10.1038/s41598-018-23930-1
- 724 51. González-González E, Mendoza-Ramos JL, Pedroza SC, Cuellar-Monterrubio AA,  
725 Márquez-Ipiña AR, Lira-Serhan D, et al. Validation of use of the miniPCR  
726 thermocycler for Ebola and Zika virus detection. Ansumana R, editor. *PLoS One*.  
727 *Public Library of Science*; 2019;14: e0215642. doi:10.1371/journal.pone.0215642
- 728
- 729
- 730
- 731
- 732

sample →

**A**

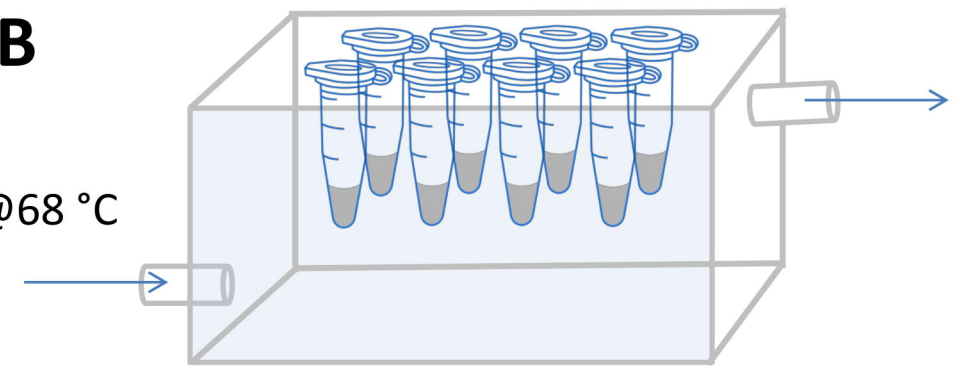


Reaction mix  
+ Primer set  $\alpha$  or  $\beta$

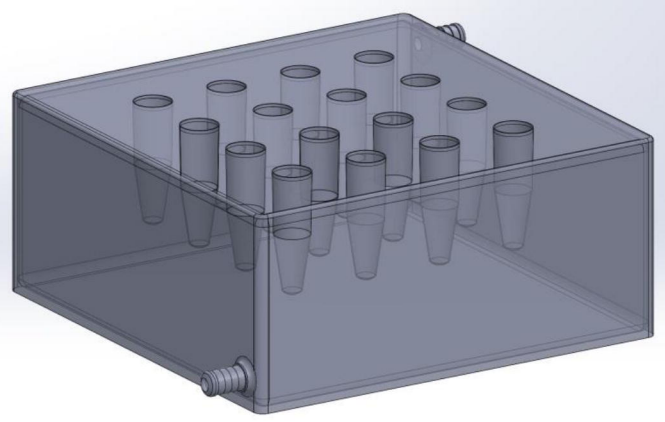
Polymerase  
Phenol red

**B**

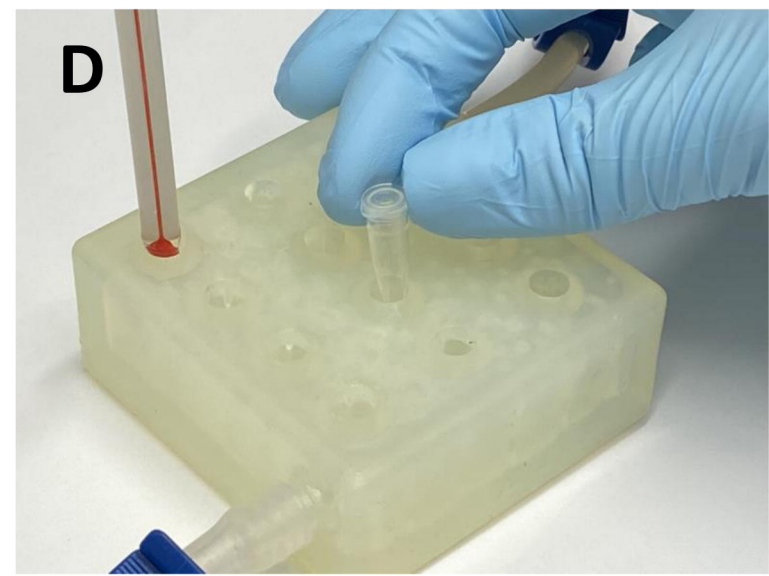
Water in @68 °C

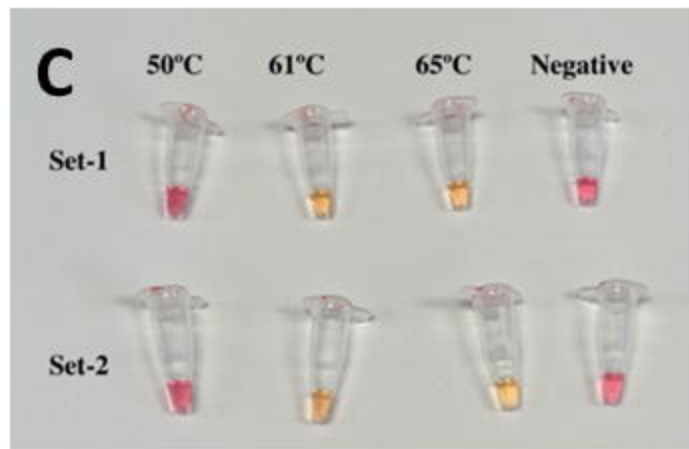
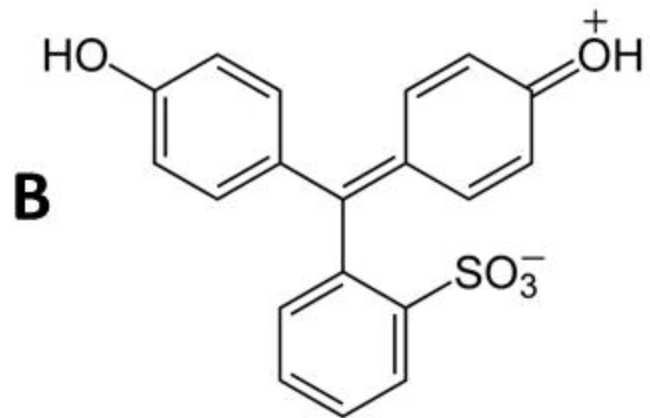
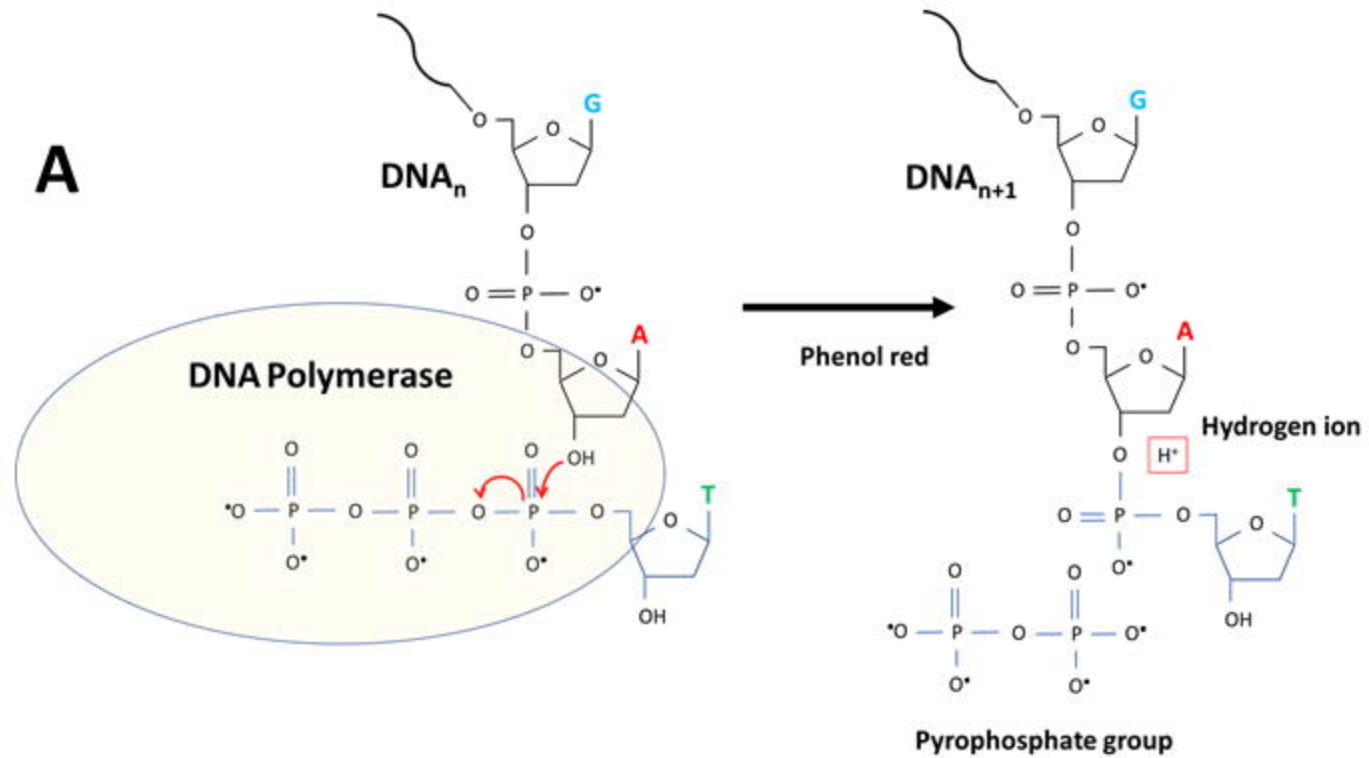


**C**



**D**





← Increasing viral copies →

**A**

$2 \times 10^5$   $4 \times 10^4$   $1 \times 10^4$   $2.5 \times 10^3$  625

**Set  $\alpha$**



**Set  $\beta$**

**B**

**Set  $\alpha$**

1 2 3 4 5 6 7

**C**

**Set  $\beta$**

1 2 3 4 5 6 7

